Evolution of the changes induced in the refractive properties of a gas by stimulated Raman scattering

M. I. Baklushina, B. Ya. Zel'dovich, N. A. Mel'nikov, N. F. Pilipetskiĭ, Yu. P. Raĭzer, A. N. Sudarkin, and V. V. Shkunov

Institute of Problems in Mechanics, Academy of Sciences of the USSR, Moscow
(Submitted March 10, 1977)
Zh. Eksp. Teor. Fiz. **73**, 831–841 (September 1977)

Laser probe signals were sent at intervals of 0.1–1 μsec along a meter-long path traversed by a strong laser pulse which produced stimulated Raman scattering in hydrogen at 10 atm. Double-exposure holographic interferometry was then used to determine the advance in the phase of the probe signal, and hence to investigate the evolution of the refractive properties of the gas in which molecular vibrations were excited. The refractive index initially increased along the path as a result of the increase in the polarizability of the molecules when vibrations were excited in them, and focusing of the radiation took place. The measured increase in polarizability was $\Delta\alpha = (1.53 \pm 0.22) \times 10^{-25}$ cm^3. This was followed by the relaxation of vibrations accompanied by thermal expansion of the gas and the defocusing of radiation which increased with time. The power of the equivalent lens producing the same focusing and defocusing effects was measured. Photographs showing the convergence and divergence of the light rays were also obtained.

PACS numbers: 51.70.+f

1. INTRODUCTION AND OBJECTIVES

It is well known (see, for example, the review by Bloembergen[1]) that stimulated Raman scattering (SRS) takes place when a sufficiently strong light beam is introduced into a molecular medium. Some of the incident quanta $\hbar\omega_L$ are transformed into the quanta of scattered Stokes radiation $\hbar\omega_S$ and these propagate in the direction of the incident beam. The energy difference $\hbar(\omega_L - \omega_S)$, which is equal to the vibrational quantum of the molecules $\hbar\Omega$, is expended in vibrational excitation.

The appearance of a large number of vibrationally excited molecules produces a change Δn in the refractive index along the beam path, and this gives rise to the refraction of the transmitted radiation. The vibrational excitation is accompanied by an increase in the polarizability of the molecules, the refractive index along the beam path becomes greater than elsewhere, and this produces a focusing effect in relation to both the incident and forward-scattered radiation. This process of self-interaction of radiation is called SRS self-focusing. It has been extensively investigated both theoretically and experimentally.[2–10]

SRS is usually excited by a giant laser pulse of length of the order of 10^{-8} sec. This excitation is followed by a much more prolonged variation in the optical (refractive) properties of the medium along the beam path. The vibrational energy is transformed into the translational energy of the moving molecules in the course of their vibrational relaxation. This type of "nonlinear" heating of the medium is frequently much greater than heating due to ordinary (linear) absorption. It is accompanied by thermal expansion and, in most media, a reduction in the refractive index. If the radiation producing the SRS were not restricted to a short pulse but were to continue, the SRS self-focusing effect would eventually necessarily be replaced by defocusing. This reversal of the focusing mechanism was investigated theoretically by Raĭzer[11] in relation to the Kerr self-focusing and thermal defocusing due to ordinary absorption of light. The result of the change in the sign of the refraction effect of SRS has been observed in experiments[8–10] on the excitation of SRS by a train of short pulses in a cell with parallel windows. SRS self-focusing was found to lead to the decollimation of the beam and a deterioration in the Q of the "resonator" for the Stokes radiation, which was formed by the reflecting windows of the cell. The result of this was an increase in the threshold, and SRS was produced by only some of the pulses in the train, separated by a "dead interval." Kravtsov, Naumkin, and Protasov[9] interpreted and qualitatively explained the size of the "dead interval" by assuming that the beam was recollimated and the Q of the resonator was reestablished when the reduction in the refractive index connected with thermal expansion was compensated by its increase due to higher polarizability.

We have used the following method for the direct experimental investigation of the evolution of the refractive properties of the medium during the excitation of SRS. A powerful giant pulse was used as the vibrational pump, and the evolution of the optical properties of the medium along the path of the beam was observed with the aid of low-power laser probe pulses sent along the same path at relatively long intervals of time, beginning with the onset of the vibrational excitation but prior to the onset of relaxation.

In contrast to previous work in which SRS self-focusing was investigated, we have examined not only the resultant effect of the change in the angular properties of the light beam, but also the changes in the refractive properties of the medium along the beam path. This was done by the method of holographic interferometry. The probe beam was used to record at each instant of time the radial distribution of the advance in the phase, or the optical length of the disturbed part of the path.

 0038-5646/77/4603-0436$02.40

As far as we know, this is the first direct determination of the time- and space-resolved disturbances in the optical properties along the beam path. To investigate the beam path at different instants of time, a new pulse was produced each time although there is a very interesting theoretical proposal for the continuous holographic recording of the entire nonstationary process during a single pump pulse.[12]

The medium under investigation was hydrogen at a pressure of 10 atm. The hydrogen molecule has a very large vibrational quantum ($\hbar\Omega = 8.75\times10^{-20}$ J, $\hbar\Omega/k$ = 6350 °K) so that one expects higher temperatures and greater thermal expansion. The relatively high pressure must be used to reduce the SRS threshold. The evolution of the refractive properties of the medium was followed for 4.5 μsec after the pump pulse. These data were then used to determine the increase in polarizability of the hydrogen molecule due to vibrational excitation, and the power and position of the "SRS lens" at different instants of time, i.e., the equivalent lens producing the same focusing or defocusing effect as the actual disturbances of the optical properties along the beam path. The experiments revealed a more rapid increase in the defocusing effect of the disturbances than one would expect from published data on vibrational relaxation in hydrogen. This is probably connected with accelerated relaxation due to impurities in the gas.

2. APPARATUS AND EXPERIMENTAL METHOD

The apparatus is illustrated schematically in Fig. 1. SRS was excited by a neodymium laser consisting of a master oscillator and two amplifiers. It was Q-switched with a Pockels cell. The master oscillator was operated in a single transverse mode. The radiation was linearly polarized. The output parameters of the laser pulse were as follows: peak power up to 20 MW, full width at half height 25–30 nsec, and divergence 0.0015–0.002 rad (determined from diffraction-intensity zeros). The radiation was focused at the midpoint of the cell filled with hydrogen at 10 atm by a lens with a focal length of 200 cm. The cell length was 122 cm. A Faraday shutter was used to prevent back-reflected radiation from entering the laser. The Faraday

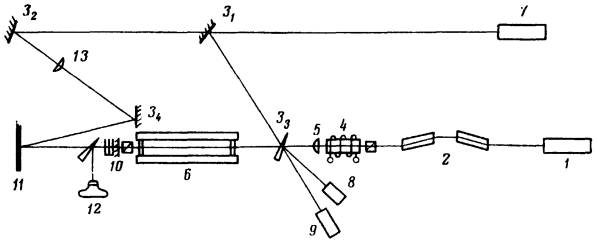

FIG. 1. Experimental arrangement: 1—exciting neodymium laser, 2—neodymium amplifier, 3—mirrors, 4—Faraday shutter, 5—focusing lens f = 200 cm, 6—cell containing compressed hydrogen, 7—probing ruby laser, 8—calorimeter for measuring the SRS pump energy, 9—photocell with oscillograph used to measure the time difference between pump and probe, 10—optical system for isolating the probe radiation, 11—holographic photofilm, 12—camera for recording the shadow pattern, 13—lens, f = 10 cm.

shutter consisted of TF-5 glass in a pulsed magnetic field and a polarizer. The shutter transmitted less than 1% of the reflected radiation into the laser.

A 10-kW ruby laser, which produced no additional disturbance in the gas, was used to probe the path traversed by the exciting laser beam. The ruby laser was Q-switched with a Pockels cell and was operated in a single mode (in the transverse and longitudinal indices). The pulse length was 40 nsec and the spectral width was 0.0005–0.001 Å. The probing pulse was synchronized with the exciting pulse with the aid of Pockels cells. The time shift between the pulses could be varied between −100 and +100 μsec. A system of mirrors and beam splitters was used to divide the probing laser beam into two. One of the two (the object beam) propagated along the path 3_1–3_3 and, having traversed the path of the exciting beam, eventually reached the holographic photofilm 11. The other (reference) beam reached the photofilm along 3_1–3_2–3_4–11. The probe beam was not focused and remained parallel to within its natural divergence.

To obtain a high-quality interference pattern from a phase object, it is essential to exclude all possible phase distortions due to optical elements and to image on the photographic film only the interfering field corresponding to the position of the phase object. Conventional interferometers do not satisfy both requirements under the conditions of stimulated Raman scattering in compressed gases. In particular, the position of the SRS lens may change radically for small changes in the energy of the exciting radiation. We used double-exposure holographic interferometry to overcome these two difficulties in conventional systems. The interference pattern is first produced without the exciting pulse and then again with the exciting pulse. This enables us to exclude distortions due to the passage of the beam through the optical element of the system (see, for example, Collier[13]).

The changes in the refractive index are very small, and the path difference between the reference and object beams is of the order of a wavelength. In conventional double-exposure interferometry, only one or two interference fringes are therefore produced and this makes it difficult to obtain information on the transverse distribution of the advance in phase. The mirror 3_4 was therefore rotated through a small angle between exposures, so that the reference beam was itself rotated for the second exposure relative to the reference beam in the first exposure. Since the hologram was reconstituted with a single beam, the reconstituted wave fronts propagated at a small angle to one another. The interference pattern therefore had a banded structure (as in conventional interferometry). This resulted in an increase in both the resolving power and the sensitivity with which the phase was recorded. Both holograms and ordinary photographs of the objects were recorded. Because of its high sensitivity, the method can be used to show directly the nature of the deviation of the probing radiation produced by the object.

The measurements were carried out along the excit-

ing beam path, so that we had the problem of isolating the probing radiation. Glass light filters could not be used to isolate the required wavelength because absorption of the entire energy of the exciting beam produced parasitic changes in the phase of the probing beam. Attempts to reflect the exciting radiation with a dielectric mirror were not successful because optical breakdown was found to occur near the mirror surface. We therefore used exciting and probe beams of different polarization. Some of the radiation energy was removed by a polarizer (stop), and the remaining small fraction was reflected by a mirror and absorbed by light filters.

The energy of the exciting pulse was measured calorimetrically in each case. The time difference between the exciting and probe pulses was measured with a photocell and an oscillograph.

3. EXPERIMENTAL RESULTS

To obtain the distribution of the advance in phase over the transverse cross section, the plane of the object must be imaged on the recording photographic film. Since a considerable length is necessary for SRS to develop, the photographic film cannot be placed directly after the object under investigation. Over long paths, on the other hand, the initial phase shift gives a considerable change in both phase and amplitude of the probe wave front in the plane of the photographic film. This ensures that the variation in the refractive index

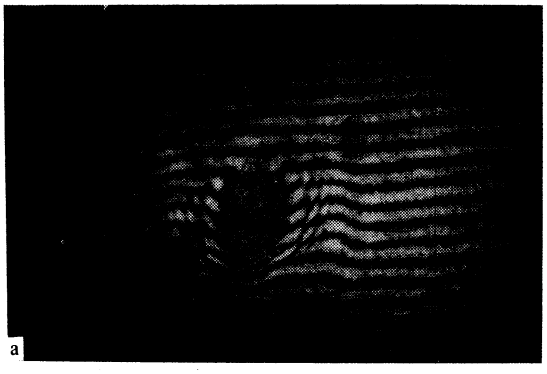

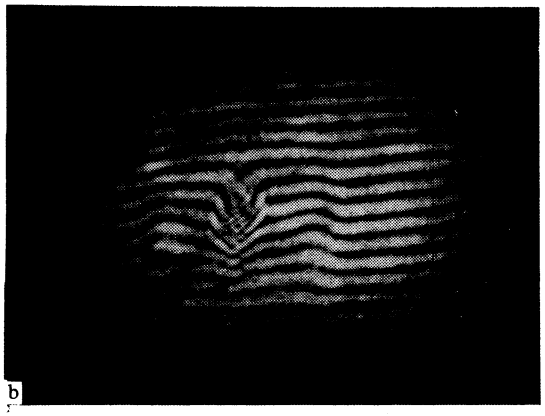

FIG. 2. Interference pattern ($t = 1.5$ sec): a—in the plane of the hologram, b—in the plane of maximum contrast of the interference fringes.

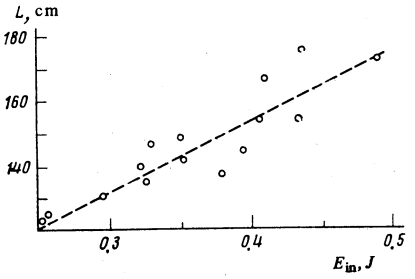

FIG. 3. Distance between the phase inhomogeneity and the hologram as a function of the energy of the exciting radiation.

is a maximum at the center of the object, and the interference fringes are found to be completely smeared out. In the process of reconstruction, we therefore photographed the plane in which the contrast of the interference fringes was a maximum. Figure 2 shows the interference pattern in the plane of the hologram and in the plane with maximum contrast of the interference fringes. It is easily seen that this plane corresponds to the plane immediately after the optical inhomogeneity, where the phase shift has not as yet affected the amplitude distribution of the probe beam. Simple formulas can then be used to determine the approximate position of the phase inhomogeneity under investigation. Figure 3 shows a graph of the position of the object under investigation as a function of the incident energy (the distance between the object and the hologram is plotted along the ordinate axis).

The distance between the hologram and the object cannot be determined with great accuracy (in the final analysis, the precision depends on the gradient of the refractive index) and the graph must be regarded as largely qualitative. Nevertheless, it shows that the distance between the object and the hologram increases with increasing incident energy, i. e., it approaches the focusing lens. This explains the fact that SRS develops at shorter distances from the beginning of the cell for stronger pump pulses.

Figure 4 shows photographs illustrating the phase changes in the probe wave front at difference instants of time for roughly the same energy of the exciting radiation (0.4 J). Figure 4b gives the corresponding photographs illustrating the amplitude variations of a plane probe wave front due to these phase changes. It is clear that the phase changes and hence their effect on the plane probe wave front are very dependent on the delay time. During the initial stage, for times $t \lesssim 0.1$ μsec, i. e., in fact, directly after the excitation of SRS, the change Δn in the refractive index is positive and the interference fringes bend upward. The intensity at the center of the photograph is somewhat higher than in the peripheral region. This is connected with some focusing of the probe radiation due to the increase in the refractive index along its path. At subsequent times, the picture undergoes a radical change. Even after 0.3 μsec, the transverse gradient of the refractive index changes sign near the beam axis, the interference fringes bend downward, and the intensity

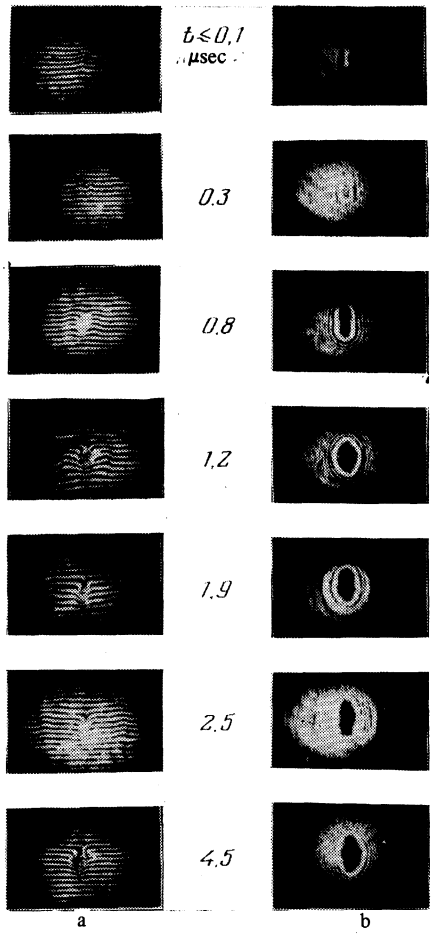

FIG. 4. Dynamics of the SRS lens: left—interference patterns; right—shadow photographs.

of the radiation falls sharply in the central part of the photograph, i. e., the axial part of the radiation is defocused. The defocusing effect increases with increasing time and substantially exceeds the initial focusing effect. During the reduction in the refractive index, waves corresponding to higher values of the refractive index propagate away from the axis in the central part of the beam. On the interference pattern, these correspond to fringes bending upward whilst, on the photographs, they correspond to regions of increased brightness. Measurements on the interference patterns show that the radial propagation velocities are in good agreement with the velocity of sound in hydrogen ($a = 1.25$ km/sec $= 1.25$ mm/μsec). These are radial compression waves due to thermal expansion of the gas in the axial region.

The interference pattern provides information on the advance in the phase of the probe wave that has traversed the region with disturbed refractive index. Consider a rectangular coordinate frame x, y, z with the light beam lying along the z axis. The advance in the phase of the light wave at the point x, y at exit from the disturbed region is

$$\Delta\varphi(x,y)=\frac{2\pi}{\lambda}\int\Delta n(x,y,z)\,dz, \qquad (1)$$

where λ is the wavelength of the probe radiation in vacuum. The vertical shift of a fringe segment by an amount equal to the separation between the fringes corresponds to $\Delta\varphi = 2\pi$ or

$$\int\Delta n\,dz=\lambda.$$

In general, it is clear from the photographs that the beam cross section is elliptical, but we shall replace it approximately by an equivalent circle. For small radial distances r from the beam axis, the advance in the phase can be approximated by the parabola

$$\Delta\varphi(r)=\Delta\varphi(0)-\frac{2\pi}{\lambda}Ar^2. \qquad (2)$$

The coefficient A is determined by the curvature of the interference fringes near the beam center if the fringes bend upward ($A>0$), and vice versa. The surface of constant phase corresponding to (2) near the axis of the light beam is part of the sphere $z = Ar^2$ + const. The rays are focused at the center of the sphere, and the focal length of the equivalent lens is equal to the radius of curvature of the spherical surface,[1)] i.e., $f = A/2$. The SRS lens powers determined in this way and the corresponding focal lengths are as follows:

t, μsec:	0.1	0.3	0.65	0.9
$1/f$, m^{-1}:	1.9	−3.2	−6.7	−10.4
f, cm:	53	−31	−15	−9.6

These data refer to the case where the energy $E_S \approx 40$–50 mJ is transferred from the pump pulse to the Stokes radiation. Positive signs correspond to focusing and negative signs to defocusing lenses.

It is clear that SRS self-focusing is rapidly transformed into defocusing, and the latter is very strong, exceeding the focusing effect by an order of magnitude after only one microsecond.

4. DETERMINATION OF THE POLARIZABILITY OF AN EXCITED HYDROGEN MOLECULE

The positive change in the refractive index of the gas during the initial stage ($t \lesssim 10^{-7}$ sec) is connected exclusively with vibrational excitation of the molecule. The variation in the advance of the phase during this stage can be used to determine directly the polarizability of the vibrationally excited molecules (α^*) or, more precisely, the difference $\Delta\alpha = \alpha' - \alpha$, where α is the polarizability of undisturbed molecules. In point of fact, if N^* is the density of excited molecules, then $\Delta n = 2\pi\Delta\alpha N^*$. Substituting this in (1) and integrating the advance in phase $\Delta\varphi(x, y)$ with respect to the transverse coordinates x, y, we obtain the total number of excited molecules throughout the excited volume:

$$\mathcal{N}^*=\int N^*dxdydz. \qquad (3)$$

On the other hand, if we neglect the excitation of the higher Stokes and anti-Stokes components, as well as the absorption of the Stokes radiation in the medium, which can be done with very little loss of accuracy, the number of excited molecules is determined simply by

the energy E_S of the emerging Stokes radiation, which can also be determined experimentally: $\mathcal{N}^* = E_S/\hbar\omega_S$. The increase in polarizability is then given by

$$\Delta\alpha = \frac{\lambda}{(2\pi)^2}\frac{\hbar\omega_S}{E_S}\int \Delta\varphi(x,y)\,dxdy. \tag{4}$$

When the advance in phase was integrated with respect to the transverse coordinates, the interference pattern was processed with allowance for the elliptic shape of the beam. This yielded $\Delta\alpha = (1.7 \pm 0.25)\times 10^{-41}$ A · sec · $m^2/V = (1.53 \pm 0.22)\times 10^{-25}$ cm^3, which amounts to 19% of α. We note that for the typical values E_S = 40 mJ and $\hbar\omega_S = 1.0\times 10^{-9}$ J, the total number of excited molecules is only $\mathcal{N}^* = 4\times 10^{17}$. The relatively low precision with which $\Delta\alpha$ was determined was due to the fact that the energy E_S of the Stokes radiation was determined from a calibration graph giving E_S as a function of the pump energy E_L. Unfortunately, the energy measurements were subject to a considerable spread. To reduce this spread, the calorimetric measurements were carried out immediately before the measurements of the refractive index, and the latter were carried out without any change in the experimental arrangement. Stimulated scattering of the higher Stokes and anti-Stokes components (up to three components were scattered) could not introduce a large error into the measured values of $\Delta\alpha$. The results obtained for $\Delta\alpha$ were, in fact, in satisfactory agreement (to within experimental error) with other measurements[7] and calculations[3] [$\Delta\alpha = (1.2 - 1.8)\times 10^{-41}$ A · sec · m^2/V and $\Delta\alpha = 1.55\times 10^{-41}$ A · sec · m^2/V, respectively].

5. THERMAL EXPANSION AND SRS DEFOCUSING

Let us now estimate the concentration of excited molecules and the temperature of the heated gas when the vibrational energy is transformed into heat. The intensity I_S of the Stokes wave increases along the path of the parallel pump beam (along the z axis) in accordance with the expression[1]

$$I_S = \frac{I_L^0}{1+(I_L^0/I_S^0)\exp(-GI_L^0 z)}, \tag{5}$$

where I_L^0 is the intensity of the pump wave at entry to the scattering medium ($z = 0$), I_S^0 is the intensity of the spontaneous Stokes radiation with which amplification begins, and G is the proportionality constant in the gain coefficient GI_L. The Stokes wave saturates over an effective distance z_{eff} which is defined by the condition $GI_L^0 z_{eff} \approx \ln(I_L^0/I_S^0)$. The distribution of the excited atoms along the direction of the beam is $N^*(z) \sim dI_S/dz$. It has a maximum at $z = z_{eff}$, and the full width of the maximum at half height is $\Delta z = 3.35/GI_L^0$. This may be adopted as the effective length of the cylinder in which the excited atoms are localized.

It is usually considered that $GI_L^0 z_{eff} \approx 20$ at the threshold intensity of the parallel pump bearer.[1] In our experiments, the beam exciting the SRS was focused with a long focal length lens and was almost parallel. The intensity on the window of the cell was measured and was found to be only half the intensity at the focus at the center of the cell. This means that, under the threshold conditions, the effective length z_{eff} is roughly equal to the length of the cell (122 cm). The intensity of the exciting radiation was greater by a factor of 1.5 than the SRS threshold, so that z_{eff} was smaller than the length of the cell by the same factor. Hence, $z_{eff} \approx 80$ cm and $z \approx 0.17 z_{eff} = 14$ cm.

The advance in the phase along the beam axis during the SRS stage gives the quantity

$$\int N^* dz \approx N^* \Delta z$$

along the beam axis. For the first interference pattern (Fig. 4a), the change of phase at the center of the beam is $\Delta\varphi \approx 0.6\times 2\pi$ and hence $N^*\Delta z \approx 0.6\lambda/2\pi\Delta\alpha \approx 4.4\times 10^{19}$ cm^{-2}. The mean density is, therefore, $N^* \approx 3.1\times 10^{18}$ cm^{-3}. The effective cross-sectional area of the column in which the excitation took place is $S = \mathcal{N}^*/N^*\Delta z \approx 0.9\times 10^{-2}$ cm^2. The cross section of the pump beam has the form of an ellipse with semiaxes in the ratio 3 : 1. The two radii of the excited column were found to be $R \approx 0.31$ mm and 1 mm.[2)] The beam radius can be measured directly from the first interference pattern, taking into account the magnification, and is given by the horizontal half-width of the central "hump." The density of molecules at $p = 10$ atm is $N = 2.7\times 10^{20}$ cm^{-3}, i.e., the concentration of excited molecules in the column, $N^*/N \approx 1.2\times 10^{-2}$, is very high.

According to recent data,[14-17] the vibrational relaxation time in hydrogen at room temperature ($T = 239$ °K), reduced to the pressure $p = 10$ atm, is $\tau \approx 35$ sec. As we shall see presently, for $t \ll \tau$, the gas is heated only a few degrees. The relaxation time τ is thus reduced only slightly, and the rate of release of heat remains constant in time. The increase in the temperature of the gas (diatomic gas, specific heat at constant pressure) is

$$\Delta T = \Delta T^\infty \frac{t}{\tau}, \quad \Delta T^\infty = \frac{N^*\hbar\Omega}{7kN/2} \approx 21°, \tag{6}$$

where ΔT^∞ corresponds to the end of vibrational relaxation ($t = \infty$).

A simple estimate of the change in the concentration of the molecules, ΔN, and the corresponding change in the refractive index, Δn_ρ, due to thermal expansion can easily be obtained on the assumption that the expansion process occurs under steady conditions at constant pressure. In this approximation,

$$\Delta n_\rho = 2\pi\alpha\Delta N = 2\pi\alpha\left(\frac{\partial N}{\partial T}\right)_p \Delta T = -2\pi\alpha N\Delta T^\infty \frac{t}{\tau}. \tag{7}$$

According to (6) and (7), the ratio of the refractive-index changes Δn due to thermal expansion to the increase in polarizability ($\Delta n_\alpha = 2\pi\Delta\alpha N^*$) is given by

$$\frac{\Delta n_\rho}{\Delta n_\alpha} = -\frac{\alpha}{\Delta\alpha}\frac{\hbar\Omega}{7kT/2}\frac{t}{\tau} \approx -33\frac{t}{\tau}. \tag{8}$$

This shows that the defocusing effect of negative Δn_ρ may exceed the focusing effect of positive Δn_α in a time $t \approx \tau/33 \approx 1$ μsec. This is an order-of-magnitude estimate, but experiments have shown that the defocusing of the axial part of the light beam sets in before this time, i.e., for $t \approx 0.2$ μsec (see above). When $t \approx 1$ μsec, defocusing is already greater than the initial focusing. The nonsteady character of the true thermal expansion process must, at least to some extent, have an effect here and should be appreciable for times t comparable with the time $t_s = R/a \approx 0.25$ μsec, i.e., the time taken by sound to traverse the characteristic distance (equal to the radius of the column in which the release of heat takes place).

The thermal expansion of the gas at low rates of heating is described by the equations of gas dynamics in the acoustic approximation. Assuming that the process is cylindrically symmetric, these equations are [11]

$$\frac{\partial \Delta\rho}{\partial t} + \rho_0 \frac{1}{r}\frac{\partial}{\partial r} ru = 0,$$
$$\rho_0 \frac{\partial u}{\partial t} + a^2 \frac{\partial \Delta\rho}{\partial r} = -\frac{\partial p_{th}}{\partial r}, \quad p_{th} = (\gamma-1) N^*(r) \hbar\Omega \frac{t}{\tau}, \tag{9}$$

where ρ_0 is the undisturbed gas density, $\Delta\rho$ is the change in density, u is the mass velocity, p_{th} is the increase in pressure due to the release of heat without change in density, and $\gamma = 7/5$ is the adiabatic exponent. In the limit as $t \gg t_s$, the pressure becomes uniform, $\partial u/\partial t \approx 0$, and $\Delta\rho \approx -p_{th}/a^2$, which is equivalent to (7).

In the opposite limiting case, when $t \ll t_s$ in the column in which the heat release takes place, we can neglect the term $a^2 \partial \Delta\rho/\partial r$. This yields [11]

$$\Delta\rho = \Delta\rho^\infty(0) \frac{t^3}{t_s^2 \tau} F(r); \quad F = \frac{1}{6}(f'' + f'/\xi), \quad \xi = r/R,$$
$$f(\xi) = N^*(r)/N^*(0), \quad \Delta\rho^\infty(0) = -(\gamma-1) N^*(0) \hbar\Omega/a^2, \tag{10}$$

where $\Delta\rho^\infty(0)$ is the final change in the density on the axis for $t = \infty$. In contrast to the quasiequilibrium case for which $\Delta\rho \sim N^* \sim f$, the distributions of $\Delta n_\rho \sim \Delta\rho$ and $\Delta n_\alpha \sim N^*$ for $t < t_s$ are given by the different functions $F(\xi)$ and $f(\xi)$. It is readily seen that, for distributions that fall with distance from the axis, say, $f = \exp(-\xi^2)$ or $\cos(\pi\xi/2)$, the expansion of the gas near the axis is greater than in peripheral regions. This is due to the fact that the mass expelled from the center, where the heat release is at a maximum, does not succed in reaching "infinity," as in the "equilibrium" case, but is mixed into the peripheral region where it partly compensates the local gas expansion.

The deviation of the light rays is determined by the radial gradient of the resultant refractive index, i.e., by the distribution

$$\Delta n = \Delta n_\rho + \Delta n_\alpha = -C_1 t^3 F\left(\frac{r}{R}\right) + C_2 f\left(\frac{r}{R}\right), \tag{11}$$

where C_1 and C_2 are coefficients independent of r and t. If the distributions F and f were identical, as in the equilibrium case, the transformation of the positive SRS lens, corresponding to the reduction in Δn between the axis and the edge, into a negative lens (Δn increases with distance from the axis) would occur simply when the change in the sign of Δn took place. If, on the other hand, the ratio F/f increases with decreasing distance from the axis, the curvature of $\Delta n(r)$ at the point $r = 0$ may change sign before the quantity Δn itself changes sign. This means that the "paraxial" lens will begin to scatter well before thermal expansion compensates the polarization effect at all points, i.e., before the time predicted by (8). Calculations with a Gaussian profile f have shown that the change in the signs of the curvature of Δn on the axis and the paraxial SRS lens occurs for

$$t \geqslant \left[\frac{3}{4}\frac{7kT/2}{\hbar\Omega}\frac{\Delta\alpha}{\alpha} t_s^2 \tau\right]^{1/3}.$$

For $R = 0.3$ mm, $t_s = 0.25$ μsec, and $\tau = 35$ μsec, we obtain $t \approx 0.33$ μsec instead of the 1 μsec predicted by (8). Admittedly, t is then somewhat greater than t_s, whilst the approximation defined by (10) is valid only for $t < t_s$, but the qualitative effect of the acceleration of the change in the sign of the lens due to nonsteady expansion processes is present.

The importance of hydrodynamic effects is also indicated by the clearly observable fact that the "positive humps" on the interference patterns (regions with $\Delta n > 0$) propagate with the velocity of sound outside the thermal column. The shift of the interference fringes in the upward direction in the "hills" is of the order of the downward shift in the "valley" at the center for $t \approx 1$ μsec, and becomes relatively smaller for times $t \approx 2$–2.5 μsec. This is consistent with the overall picture of the process. For $t \sim t_s$, the gas injected from the thermal column is concentrated not too far from its boundary, the cylindric factor still has a relatively minor effect, and $\Delta\rho$ in the compression region is of the same order as on the axis where expansion takes place. For $t \gg t_s$, the compression wave departs with the velocity of sound to considerable distances, and the mass $M \sim \pi R^2 |\Delta\rho(0)|$ ejected per unit length of the column is distributed over a volume of the order of $\pi(at)^2$, i.e., the increase in density in the compression wave is of the order of $\Delta\rho \sim |\Delta\rho(0)| (t_s/t)^2 \ll |\Delta\rho(0)|$.

It is important to note that the photographs in Fig. 4b can be used independently of the interference patterns to estimate the variation in the refractive index along the beam path. The radius r_1 of the dark spot and the distance L between the photographic film and the disturbed region in the cell can be used to determine the angle of deflection $\theta \approx r_1/L$ of the parallel probe beam in the axial region, due to the appearance of negative values of Δn. Thus, for $t = 0.8$ μsec, $r_1 = 1.6$ mm, and $L \approx 120$ cm, we have $\theta \approx 0.00135$. In the case of small deflections, the ray equations given by geometric optics yield $\theta = (2|\Delta n'|)^{1/2}$, where $\Delta n'$ is the radial difference between the refractive indices "traversed" by the beam in the course of its deflection from the initial direction along the z axis. [11] A path length $\Delta z \approx 14$ cm in the medium corresponds to a radial deviation of the axial part of the beam through a distance $\Delta r \approx \theta \Delta z \approx 0.19$ mm, which is comparable with the radius $R \approx 0.3$ mm of the disturbed column, but is still less

than this radius. Since at time $t \approx 0.8$ μsec, $|\Delta n_\rho|$ is comparable with Δn_α, one would expect that $\Delta n' = \Delta n'_\alpha - |\Delta n'_\rho|$ would be of the order of $\Delta n_\alpha = 2\pi\Delta\alpha N^*$, but less than this quantity. In fact, $\Delta n' = -\theta^2/2 \approx -0.9 \times 10^{-6}$ and $\Delta n_\alpha \approx 3 \times 10^{-6}$.

Let us now summarize our discussion. It must be admitted that, despite the qualitative agreement between experiment and the above discussion of the hydrodynamic process, a quantitative analysis of the latter, based on various approximations and the solution of a number of model problems, does not yield a satisfactory explanation of the measured absolute advances in the phase and the powers of the SRS lenses during the thermal expansion process. Theoretical calculations can be made to agree with experiment only if it is assumed that thermal expansion occurs more rapidly than is indicated by the vibrational relaxation time $\tau \approx 35$ sec. In fact, our values of τ are smaller than this value by factors of two or three. It is very likely that this is a reflection of the true state of affairs. Although published data[14–17] provide no indication of the purity of the hydrogen gas employed, it is probable that high-purity gas was employed as is customary in studies of vibrational relaxation because fractions of a percent of water vapor or organic molecules produce considerable acceleration of vibrational relaxation. On the other hand, our experiments were performed with ordinary commercial hydrogen and the cell was not specially cleaned. This was probably the reason for the acceleration of relaxation.

In conclusion, the authors wish to thank V. F. Strel'tsov for his help in the preparation of the experiment, and Yu. G. Khronopulo and V. P. Protasov for valuable discussions.

[1)]For example, if the light beam passes from air into a thin lens, one surface of which is a plane and the other a sphere of radius R, then $A = (n-1)/2R$, where n is the refractive index of the lens material and $f = R/(n-1)$.

[2)]We note that these values are somewhat smaller than the transverse dimensions of the beam itself. This is not unexpected because the excitation of SRS is very dependent on the pump intensity which decreases between the beam axis and its periphery.

[1]N. Bloembergen, Am. J. Phys. **35**, 989 (1967).
[2]G. A. Askar'yan, Pis'ma Zh. Eksp. Teor. Fiz. **4**, 400 (1966) [JETP Lett. **4**, 270 (1966)].
[3]B. Vil'gel'mn and É. Goĭman, Zh. Prikl. Spektrosk. **19**, 3 (1973).
[4]V. S. Butylkin. A. E. Kaplan, and Yu. G. Khronopulo, Izv. Vyssh. Uchebn. Zaved. Radiofiz. **12**, 3 (1969).
[5]V. S. Butylkin, A. E. Kaplan, and Yu. G. Khronopulo, Zh. Eksp. Teor. Fiz. **59**, 921 (1970) [Sov. Phys. JETP **32**, 501 (1971)].
[6]V. S. Butylkin, A. E. Kaplan, and Yu. G. Khronopulo, Opt. Spektrosk. **31**, 224 (1971) [Opt. Spectrosc. (USSR) **31**, 120 (1971)].
[7]V. S. Butylkin, G. V. Venkin, L. L. Kulik, D. I. Maleev, V. P. Protasov, and Yu. G. Khronopulo, Pis'ma Zh. Eksp. Teor. Fiz. **19**, 7 (1974) [JETP Lett. **19**, 3 (1974)].
[8]N. V. Kravtsov and N. I. Naumkin, Pis'ma Zh. Eksp. Teor. Fiz. **21**, 9 (1975) [JETP Lett. **21**, 4 (1975)].
[9]N. V. Kravtsov, N. I. Naumkin, and V. P. Protasov, Kvantovaya Elektron. (Moscow) **2**, 1585 (1975) [Sov. J. Quantum Electron. **5**, 864 (1975)].
[10]N. V. Kravtsov and N. I. Naumkin, Kvantovaya Elektron. (Moscow) **3**, 647 (1976) [Sov. J. Quantum Electron. **6**, 355 (1976)].
[11]Yu. N. Raĭzer, Zh. Eksp. Teor. Fiz. **52**, 470 (1967) [Sov. Phys. JETP **25**, 308 (1967)].
[12]T. I. Kuznetsova, Tr. Fiz. Inst. Akad. Nauk SSSR **84**, (1975).
[13]R. J. Collier, Optical Holography, Academic Press, New York (1971) (Russ. Transl., Mir, M., 1973).
[14]M. A. Kovacs and M. E. Mack, Appl. Phys. Lett. **20**, 487 (1972).
[15]M. M. Audibert, C. Joffrin, and J. Ducuing, Chem. Phys. Lett. **25**, 158 (1974).
[16]M. M. Audibert, C. Joffrin, and J. Ducuing, Chem. Phys. Lett. **19**, 26 (1973).
[17]M. M. Audibert, R. Vilaseca, J. Lukasik, and J. Ducuing, Chem. Phys. Lett. **31**, 232 (1975).

Translated by S. Chomet